Real-Time Speckle and Impulsive Noise Reduction in 3-D Ultrasound Imaging based on Order Statistics

Francisco J. Gallegos-Funes[1], Volodymyr I. Ponomaryov[2]

National Polytechnic Institute of Mexico
Mechanical and Electrical Engineering Higher School
[1] U. P. Zacatenco, Av. IPN s/n, Edificio Z, Acceso 3, 3er. piso; Col. Lindavista, 07738, Mexico D.F., Mexico, Phone/Fax (52-55) 5729-6000 ext. 54622, Email: fgallegosf@ipn.mx
[2] U. P. Culhuacan, Av. Santa Ana 1000, Col. San Francisco Culhuacan, 04430, Mexico D.F., Mexico, Phone/Fax (52-55) 5656-2058, Email: vponomar@ipn.mx

Abstract. This paper presents an approach based on order statistics for speckle and impulsive noise reduction in the 3-D ultrasound images. The proposed technique uses the *Rank M-type* (RM) estimators and these ones are adapted to 3-D image processing applications. The theory and the real-time implementation of such a technique are presented and verified using real clinical ultrasound images. The real-time implementation of 3-D image filtering was realized on the DSP TMS320C6711. In addition, the results from known techniques are compared with the proposed method to demonstrate its performance in terms of noise suppression, fine detail preservation, and processing time criteria.
Keywords: *Ultrasound imaging*, *Order Statistics* Filters, *RM-estimators*.

1 Introduction

The ultrasound imaging has been considered as one of the most powerful techniques for medical diagnosis and it is often prefer over other medical imaging modalities due it is noninvasive, portable, and versatile [1-6]. It does not use ionizing radiations, and is relatively low-cost. One of the areas where research in this field has addressed is the fundamental problem of speckle noise influence, which is a major limitation on image quality in ultrasound imaging [2].

Imaging speckle is a phenomenon that occurs when a coherent source and a noncoherent detector are used to interrogate a medium, which is rough on the scale of the wavelength. Speckle noise occurs especially in images of the liver and kidney whose underlying structures are too small to be resolved using long ultrasound wavelength. The presence of speckle noise affects the human interpretation of the images as well the accuracy of computer-assisted diagnostic techniques. As a result, speckle filtering is a critical pre-processing step for feature extraction, analysis, and recognition from medical imagery measurements [1, 2]. Current speckle and impulsive noise reduction methods have been addressed in medical systems and others such as remote sensing, communication, etc., to resolve the problem of noise during the acquisition and restoration of image information in three dimensions [3, 4, 7-11].

© *A. Gelbukh, C. Yáñez Márquez, O. Camacho Nieto (Eds.)*
Advances in Artificial Intelligence and Computer Science
Research on Computing Science 14, 2005, pp. 125-136

The possibility to process 3-D images presents a new application where it is necessary to improve the quality of 3-D objects inside the image, suppressing a noise of different nature (impulsive, Gaussian noise, or may be by speckle one) that always affects the communication or acquisition process [7]. Multiplicative (speckle) noise is common for any system using a coherent sensor, for example, the ultrasound transducer [2-6]. Other problem that is not trivial is the adaptation and implementation of the current filters, that have been investigated in different papers in the case of 2-D image processing to process objects in 3-D by use multiframe methods to increase the signal-to-noise ratio (SNR) [7, 12].

In this paper, we captured 3-D ultrasound images, these images are processed applying different non linear order statistics filters [8-11]. The Texas Instruments DSP TMS320C6711 was used for implementing of the algorithms and obtaining the processing time needed in the case of each a 3-D filter [13-15]. Based on the processing time values of each a 3-D filter, different configurations of sweeping cubes (voxels) were used to obtain a balance between the processing time and quality of the restoration of the 3-D images [7, 12]. The goal of this paper is the capability and real-time processing features of the robust RM-KNN (Rank M-type K-Nearest Neighbor) filters [16, 17] for the removal of speckle and impulsive noise in 3-D ultrasound images. Extensive simulation results have demonstrated that the proposed filter can consistently outperform other filters by balancing the tradeoff between noise suppression and detail preservation.

2 Proposed 3-D Filtering Scheme

In recent works [16-18], we proposed the combined RM (Rank M-type) – estimators for applications in image noise suppression. These estimators use the *M*-estimator combined with the *R*-estimator, such as the median, Wilcoxon or ABST (Ansari-Bradley-Siegel-Tukey) estimator. It was demonstrated in [16] that the robust properties of the RM-estimators exceed the robust properties of the base *R*- and *M*-estimators for the impulsive and speckle noise suppression. The RM-estimators used in the proposed 3-D filtering scheme are presented in such a form [16-18]:

$$\theta_{\text{medM}} = \text{MED}\left\{X_i \varphi\left(X_i - \text{MED}\{\mathbf{X}\}\right), i = 1,\ldots,N\right\} \tag{1}$$

$$\theta_{\text{WilM}} = \underset{i \le j}{\text{MED}}\left\{\frac{1}{2}\left[X_i \varphi\left(X_i - \text{MED}\{\mathbf{X}\}\right) + X_j \varphi\left(X_j - \text{MED}\{\mathbf{X}\}\right)\right],\ i = 1,\ldots,N\right\} \tag{2}$$

$$\theta_{\text{ABST M}} = \text{MED}\left\{\begin{array}{ll} X_i \tilde{\varphi}\left(X_i - \text{MED}\{\tilde{\mathbf{X}}\}\right), & i \le \frac{N}{2} \\ \frac{1}{2}\left[X_i \tilde{\varphi}\left(X_i - \text{MED}\{\tilde{\mathbf{X}}\}\right) + X_j \tilde{\varphi}\left(X_j - \text{MED}\{\tilde{\mathbf{X}}\}\right)\right], & \frac{N}{2} < i \le N \end{array}\right\} \tag{3}$$

where θ_{MedM}, θ_{WilM}, and θ_{ABSTM} are the Median M-type, Wilcoxon M-type, Ansari-Bradley-Siegel-Tukey M-type estimators, respectively, X_p are data samples

$p=1,\ldots,N$, φ is the normalized function ψ: $\psi(X)=X\varphi(X)$, and $\vec{X}$ is the primary data sample.

The family of RM-KNN type image filters has been designed by use the combined RM-estimators (1), (2), and (3) to increase the robustness of the KNN filter. The detail description of such a filtering scheme is presented in the recent works [16-18], and in here we proposed its modifications for 3-D imaging purposes. So, the 3-D RM-KNN (Rank M-type K-Nearest Neighbor) filters are defined in the following way:

The 3-D MM-KNN (Median M-type K-Nearest Neighbor) filter [16]

$$\hat{f}^{(w)}_{\mathrm{MMKNN}}(i,j,k)=\mathrm{MED}\left\{h^{(w)}(i+l,j+m,k+n)\right\} \tag{4}$$

the 3-D WM-KNN (Wilcoxon M-type K-Nearest Neighbor) filter [18, 20]

$$\hat{f}^{(w)}_{\mathrm{WMKNN}}(i,j,k)=\underset{l\le j}{\mathrm{MED}}\left\{\frac{h^{(w)}(i+l,j+m,k+n)+h^{(w)}(i+l_1,j+m_1,k+n_1)}{2}\right\} \tag{5}$$

and the 3-D ABSTM-KNN (Ansari-Bradley-Siegel-Tukey M-type K-Nearest Neighbor) filter [17]

$$\hat{f}^{(w)}_{\mathrm{ABSTMKNN}}(i,j,k)=\underset{l\le j}{\mathrm{MED}}\left\{\begin{array}{ll} h^{(w)}(i+l,j+m,k+n), & i,j\le\dfrac{N}{2} \\ \dfrac{h^{(w)}(i+l,j+m,k+n)+h^{(w)}(i+l_1,j+m_1,k+n_1)}{2}, & \dfrac{N}{2}<i \end{array}\right\} \tag{6}$$

where $h^{(w)}(i+l,j+m,k+n)$ and $h^{(w)}(i+l_1,j+m_1,k+n_1)$ are set of K_{close} values of voxels weighting in accordance with the used $\varphi(X)$ influence function into a rectangular 3-D grid of voxels that are closest to the estimation obtained at previous step $\hat{f}^{(w-1)}_{\mathrm{RMKNN}}(i,j,k)$. The initial estimation is $\hat{f}^{(0)}_{\mathrm{RMKNN}}(i,j,k)=x(i,j,k)$ and $\hat{f}^{(w)}_{\mathrm{RMKNN}}(i,j,k)$ denotes the estimate at the iteration w. $x(i,j,k)$ is the 3-D image contaminated by noise in the rectangular 3-D grid where i and j are the 2-D spatial axes and k is the time axis (or third dimension). The filtering 3-D grid size is $N_1\times N_2\times N_3$, $N_p=(2L+1)^2$ and $l_p,m_p,n_p=-L,\ldots,L$. $K_{close}(i,j,k)$ is the current number of the nearest neighbor voxels, it reflects the local data activity and noise presence and is determined by [16, 17]:

$$K_{close}(i,j,k)=\left\lfloor K_{min}+aD_{\eta}(i,j,k)\right\rfloor\le K_{max} \tag{7}$$

where the parameter a controls the filter sensitivity to local data variance and details detecting ability, K_{min} is the minimal number of neighbours into the 3-D grid for noise removal and K_{max} is the maximal number of neighbours into the 3-D grid for edge restriction and detail smoothing. $D_{\eta}(i,j,k)$ is the noise detector [16, 17]

$$D_\eta(i,j,k)=\frac{\mathrm{MED}\{|x(i,j,k)-x(i+l,j+m,k+n)|\}}{\mathrm{MAD}\{x(i,j,k)\}}+\frac{1}{2}\cdot\frac{\mathrm{MAD}\{x(i,j,k)\}}{\mathrm{MED}\{x(i+l,j+m,k+n)\}} \quad (8)$$

and MAD is the median of the absolute deviations from the median [9, 19].

The algorithm finishes when $\hat{f}^{(w)}_{\mathrm{RMKNN}}(i,j,k)=\hat{f}^{(w-1)}_{\mathrm{RMKNN}}(i,j,k)$ (the subscripts RMKNN denotes the MMKNN, or WMKNN, or ABSTMKNN filters). We use in the proposed 3-D filters the following influence functions [9, 16, 19]: simplest cut, Hampel's three part redescending, Andrew's sine, Tukey biweight, and Bernoulli. It was demonstrated that the use of the such influence functions can provide good suppression of speckle and impulsive noise [9, 16, 19]. We also propose for enhancement of the removal ability of MM-KNN filter in the presence of impulsive noise involving the standard median filter. The numerical simulations have shown that for $K_{close}>7$ the 3-D RM-KNN filters can be substituted by the *3x3x3 median* filter and for $K_{close}>350$ we can use the *5x5x5 median* filter [18].

Several parameters that characterize 3-D RM-KNN filters and influence functions were found after numerous simulations by means of use a 3x3x3 grid (i.e., $N_1\times N_2\times N_3=27$, $l,m,n=-1,\ldots,1$, and $N_p=(2L+1)^2=9$). The parameter a of the filters controls the noise suppression and detail preservation, and parameters of the influence functions can improve robustness of the filters [16]. We found that K_{min}=5 and K_{max}=24 for each a 3-D RM-KNN filter. The parameters of influence functions were: Simplest cut, *a=8, r=255;* Hampel, *a=8,* α=200, β=230, *r=256;* Andrew's sine, *a=10, r=255;* Tukey, *a=10, r=255;* Bernoulli, *a=10, r=255.* We noticed that there can be existed some variations of about ±(5-10)% of PSNR and MAE performances with the use of the other parameter values in comparison with applied ones, and finally, we have standardized these parameters as the constants to realize the real-time implementation of the 3-D RM-KNN algorithms.

3 Overall 3-D Filtering Performance

The objective criteria employed to compare the performance of noise suppression of proposed and comparative filters were the *peak signal to noise ratio* (PSNR) and for the evaluation of fine detail preservation the *mean absolute error* (MAE) [7-11]:

$$\mathrm{PSNR}=10\cdot\log\left[\frac{(255)^2}{\mathrm{MSE}}\right],\mathrm{dB} \quad (9)$$

$$\mathrm{MAE}=\frac{1}{N_1N_2N_3}\sum_{i=0}^{N_1-1}\sum_{j=0}^{N_2-1}\sum_{k=0}^{N_3-1}\left|S(i,j,k)-\hat{f}(i,j,k)\right| \quad (10)$$

where $\mathrm{MSE}=\frac{1}{N_1N_2N_3}\sum_{i=0}^{N_1-1}\sum_{j=0}^{N_2-1}\sum_{k=0}^{N_3-1}\left[S(i,j,k)-\hat{f}(i,j,k)\right]^2$ is the *mean square error,*

$S(i,j,k)$ is the original free noise 3-D image, $\hat{f}(i,j,k)$ is the restored 3-D image, and N_1, N_2, N_3 are the sizes of the 3-D image.

During the investigations of 3-D filtering algorithms the ultrasound images were contaminated by noise of different nature: speckle and impulsive ones. As it was mentioned before the speckle noise is natural for ultrasound transducers. So, each a 3-D ultrasound image can contain this noise. The described 3-D RM-KNN filters with different influence functions have been evaluated, and their performance has been compared with different nonlinear 2-D filters which were adapted to 3-D. The filters used as comparative ones were the *modified α-Trimmed Mean* [9, 22], *Ranked-Order* (RO) [9, 11], *Multistage Median* (MSM1 to MSM6) [23], *Comparison and Selection* (CS) [9, 11], *MaxMed* [24], *Selection Average* (SelAve) [9, 11], *Selection Median* (SelMed) [9, 11], and *Lower-Upper-Middle* (LUM, LUM Sharp, and LUM Smooth) [25] filters. These filters were computed according with their references and were adapted to 3-D imaging.

The experiment 1 was realized by degraded an ultrasound sequence of 640x480 pixels with 90 frames (3-D image of 640x480x90 voxels) with 5, 10, 15, 20, and 25% of impulsive noise and with the natural speckle noise of the 3-D image. Table 1 shows the performance results of proposed and comparative results filters applied to a frame of the original sequence by use the *xz* plane. The table shows that the better performances were obtained with the use of proposed filters when the noise level is of 15% or more. The LUM Smooth and MSM5 can preserve the edges and fine details in 3-D images for sufficiently small percentages of impulsive noise, but for higher noise levels they lose the ability to suppress a noise.

Table 1. Performance results in a frame of ultrasound sequence degraded with impulsive noise.

3-D Filters	Impulsive noise percentage									
	5%		10%		15%		20%		25%	
	PSNR	MAE	PSNR	MAE	PSNR	MAE	PSNR	MAE	PSNR	MAE
α Trimmed Mean	24.903	7.049	24.912	7.104	24.832	7.206	24.715	7.348	24.522	7.535
Ranked Order	26.502	6.672	26.449	6.745	26.376	6.834	26.279	6.942	26.136	7.084
MSM1	28.923	4.250	28.515	4.454	27.740	4.796	26.685	5.302	25.331	6.047
MSM2	28.135	5.062	27.806	5.219	27.161	5.518	26.187	6.004	24.962	6.729
MSM3	27.461	5.948	27.357	6.051	27.186	6.210	26.880	6.461	26.435	6.821
MSM4	27.942	5.331	27.828	5.403	27.570	5.557	27.134	5.809	26.467	6.207
MSM5	29.449	3.770	28.790	3.997	27.612	4.427	25.985	5.168	24.230	6.238
MSM6	28.299	5.069	28.205	5.129	27.993	5.254	27.675	5.445	27.099	5.770
MaxMed	27.104	6.240	26.227	6.833	24.902	7.774	23.248	9.204	21.532	11.190
SelAve	26.839	6.978	25.268	9.195	23.744	11.701	22.344	14.329	21.141	16.951
SelMed	27.434	5.636	27.028	5.871	26.675	6.109	26.314	6.369	25.906	6.682
LUM Smooth	29.943	2.756	28.936	3.128	27.347	3.772	25.261	4.879	23.027	6.573
LUM Sharp	17.368	17.282	16.503	18.861	16.015	19.894	15.904	20.167	16.077	19.815
LUM	18.538	15.518	18.235	16.202	17.850	17.081	17.599	17.684	17.517	17.866

MM-KNN Cut	28.836	4.277	28.519	4.562	28.225	4.847	27.919	5.136	27.590	5.457
MM-KNN Hamp.	28.790	4.314	28.480	4.596	28.193	4.878	27.890	5.164	27.567	5.484
MM-KNN Sine	28.367	4.660	28.082	4.940	27.803	5.221	27.473	5.516	27.131	5.838
MM-KNN Berno.	28.443	4.641	28.171	4.915	27.921	5.187	27.651	5.465	27.350	5.773
MM-KNN Tukey	28.433	4.643	28.158	4.919	27.904	5.192	27.619	5.474	27.311	5.785
WM-KNN Cut	22.801	10.873	22.616	11.014	22.375	11.232	22.044	11.539	21.720	11.908
WM-KNN Hamp.	22.759	10.919	22.574	11.059	22.328	11.279	21.986	11.590	21.656	11.964
ABSTM-KNN Cut	27.525	5.160	27.288	5.426	27.060	5.693	26.823	5.957	26.596	6.241
ABSTM-KNN Hamp.	27.458	5.210	27.737	5.473	27.007	5.737	26.774	5.997	26.550	6.280

Figure 1 displays the visual results in terms of restored images obtained by the use of different filters according to Table 1. In this figure one can see the better results in noise suppression and detail preservation were obtained using the proposed filters.

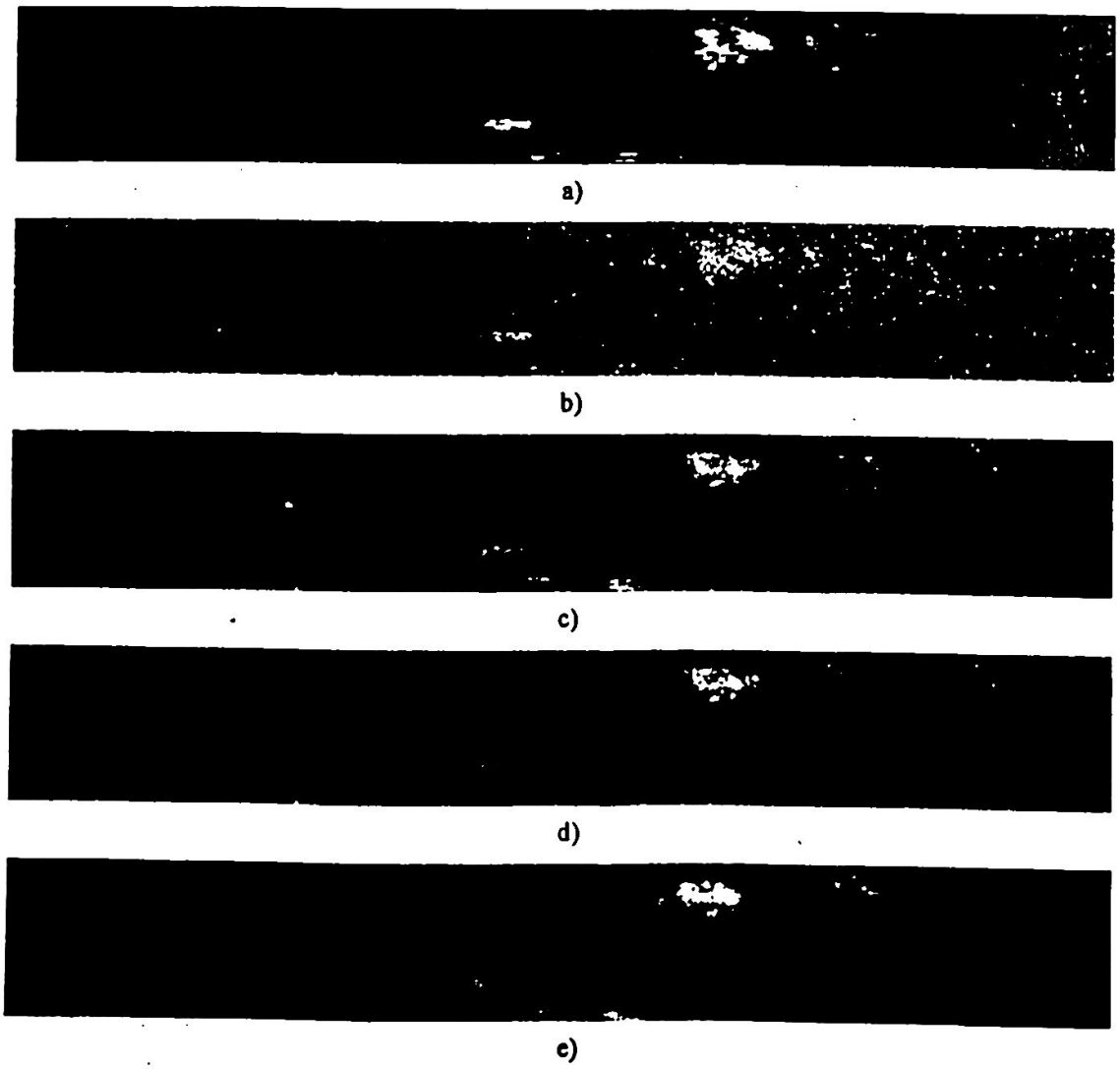

Figure 1. Visual results in a frame of ultrasound sequence. a) original image, b) image degraded by 25% of impulsive noise, c) restored image by LUM filter Smooth, d) restored image by MSM6 filter, e) restored image by filter MMKNN (Hampel).

The experiment 2 was realized in the same sequence but it was degraded with 0.05, 0.1, 0.15, and 0.2 of variance of speckle noise added to the natural speckle noise of the sequence. The performance results are depicted in Table 2 by use a frame of the sequence. From this table one can see that the 3-D MM-KNN filters provide similar results in comparison to Ranked Order and MSM filters, and in some cases the proposed filters provide better results.

Other experimental investigations were connected with different voxels cube configurations to provide better noise reduction [7, 12]. Figure 2 presents nine voxel configurations used in the proposed 3-D filtering algorithms. It is obvious that by use of less voxels in the different cube configurations the processing time is decreased.

In the experiment 3 the ultrasound sequence was degraded with 10, 20, and 30% of impulsive noise. Then, we implemented the cube configurations in the proposed filters and the α-Trimmed Mean filter. Table 3 presents the performance results of MM-KNN and α-Trimmed Mean filters in the case of use different cube configurations in the *xy* plane of the sequence. We can observe from this table that the MM-KNN filter provide better results in comparison with the α-Trimmed Mean filter. Therefore, we observe that the cubes *g* and *i* improve the noise suppression when the noise level is high, and the cubes *a* and *b* suppress efficiently the noise when the percentage of noise is small.

Table 2. Performance results in a frame of ultrasound sequence degraded with speckle noise.

3-D Filters	Speckle Noise Variance							
	0.05		0.1		0.15		0.2	
	PSNR	MAE	PSNR	MAE	PSNR	MAE	PSNR	MAE
Modified Trimmed Mean	20.418	15.124	19.095	18.663	18.245	21.257	17.621	23.327
Ranked Order	21.587	14.520	19.802	18.179	18.737	20.832	17.957	23.020
MSM1	20.568	17.624	18.061	23.684	16.592	28.104	15.589	31.521
MSM2	20.484	17.789	18.038	23.725	16.574	28.152	15.562	31.619
MSM3	22.421	14.206	20.261	18.456	18.890	21.704	17.932	24.255
MSM4	21.697	15.401	19.348	20.351	17.911	24.100	16.906	27.076
MSM5	19.554	20.207	16.964	27.444	15.478	32.608	14.431	36.801
MSM6	22.083	14.688	19.744	19.374	18.287	23.025	17.256	25.979
MaxMed	18.562	24.206	15.919	32.913	14.288	39.757	13.119	45.492
CS	15.435	32.875	13.843	39.778	13.082	43.220	12.587	45.416
SelAve	21.182	17.647	19.192	22.814	17.875	26.865	16.955	30.038
SelMed	20.836	15.750	19.013	20.094	17.870	23.300	17.029	25.969
LUMSmooth	17.915	25.142	15.440	33.823	14.001	39.991	13.010	44.771
LUMSharp	15.625	30.927	14.444	36.425	13.819	39.383	13.430	41.228
LUM	15.518	31.427	14.379	36.748	13.784	39.559	13.418	41.324
MM-KNN CUT	21.554	15.199	18.949	20.995	17.457	25.110	16.546	27.888
MM-KNN HAMPEL	21.572	15.169	19.040	20.798	17.671	24.571	16.934	26.809
MM-KNN SINE	21.399	14.614	18.640	20.226	17.101	24.310	16.048	27.474
MM-KNN BERNOULLI	22.658	13.309	20.075	17.819	18.253	21.460	16.884	24.419
MM-KNN TUKEY	22.499	13.446	19.855	18.125	18.302	21.543	17.357	23.890

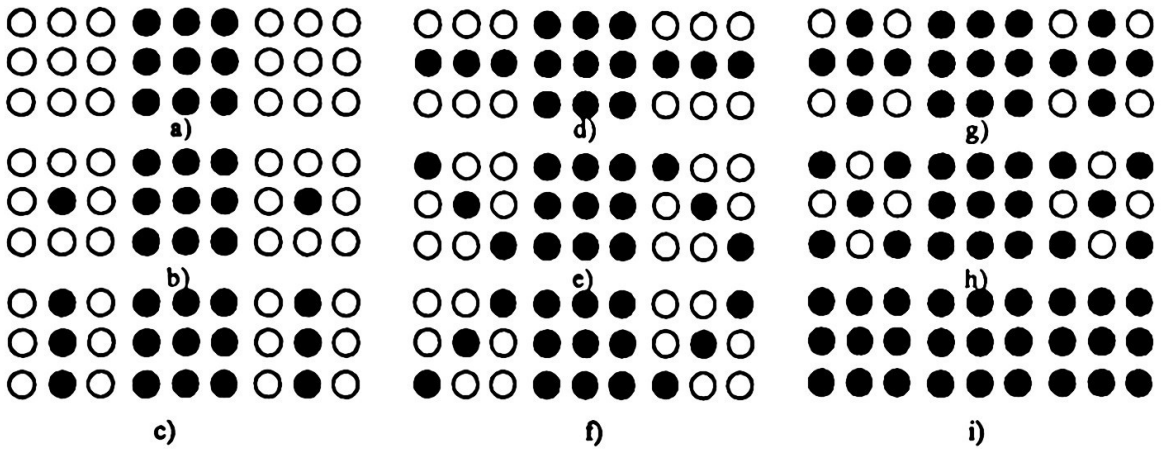

Figure 2. Different configurat' ns of processing cube.

Table 3. Performance results by use different cube configurations in a frame of ultrasound sequence degraded with impulsive noise.

Voxel configuration	Impulsive noise percentage					
	10%		20%		30%	
	MMKNN Cut Filter					
	PSNR	MAE	PSNR	MAE	PSNR	MAE
a	31.17535	3.64016	28.40849	4.53838	23.90324	6.99018
b	31.30555	3.76703	29.41062	4.41531	25.35587	6.33257
c	29.59351	4.79816	28.76898	5.28413	26.50147	6.49814
d	29.62101	4.70299	28.85542	5.15630	26.60073	6.35310
e	28.50828	4.80637	28.70908	5.28963	26.46848	6.50239
f	29.49613	4.81058	28.68377	5.29791	26.45389	6.51271
g	28.97272	4.75225	28.43172	5.23398	27.10414	6.13451
h	28.76109	4.88553	28.19258	5.38470	26.89461	6.29676
i	28.51900	4.56200	27.91900	5.13600	27.22200	5.81900
	Modified α-Trimmed Mean Filter					
a	30.07507	4.66202	26.31513	6.97970	22.28058	11.66430
b	30.85167	4.36141	28.23672	5.68776	24.16346	9.17320
c	29.63262	4.96245	28.74842	5.48613	26.13527	7.43995
d	29.73005	4.83643	28.87602	5.34850	26.23982	7.29035
e	29.53979	4.96895	28.68096	5.49478	26.09710	7.44773
f	29.51616	4.97610	28.65847	5.50289	26.08362	7.45916
g	28.65049	5.41481	28.29551	5.68411	26.86466	6.85965
h	28.40716	5.57233	28.03793	5.85165	26.64502	7.03270
i	26.03500	7.41100	25.74500	7.76400	25.21500	8.58600

Figure 3 presents the processed images by the use of MM-KNN filter with different cube configurations, in these images we observe that the MM-KNN filter provides impulsive noise suppression and detail preservation, and it can suppress the speckle noise due the ultrasound transducer.

4 Run-Time Analysis on DSP TMS320C6711

The runtime analysis of the 3-D RM-KNN filters and other concerned filters were implemented by using the Texas Instruments DSP TMS320C6711 [13]. This DSP has a performance of up to 900 MFLOPS at a clock rate of 150 MHz [13]. The filtering algorithms were implemented in C language using the BORLANDC 3.1 for all routines, data structure processing and low level I/O operations. Then, we compiled and executed these programs in the DSP TMS320C6711 applying the Code Composer Studio 2.0 [14, 15].

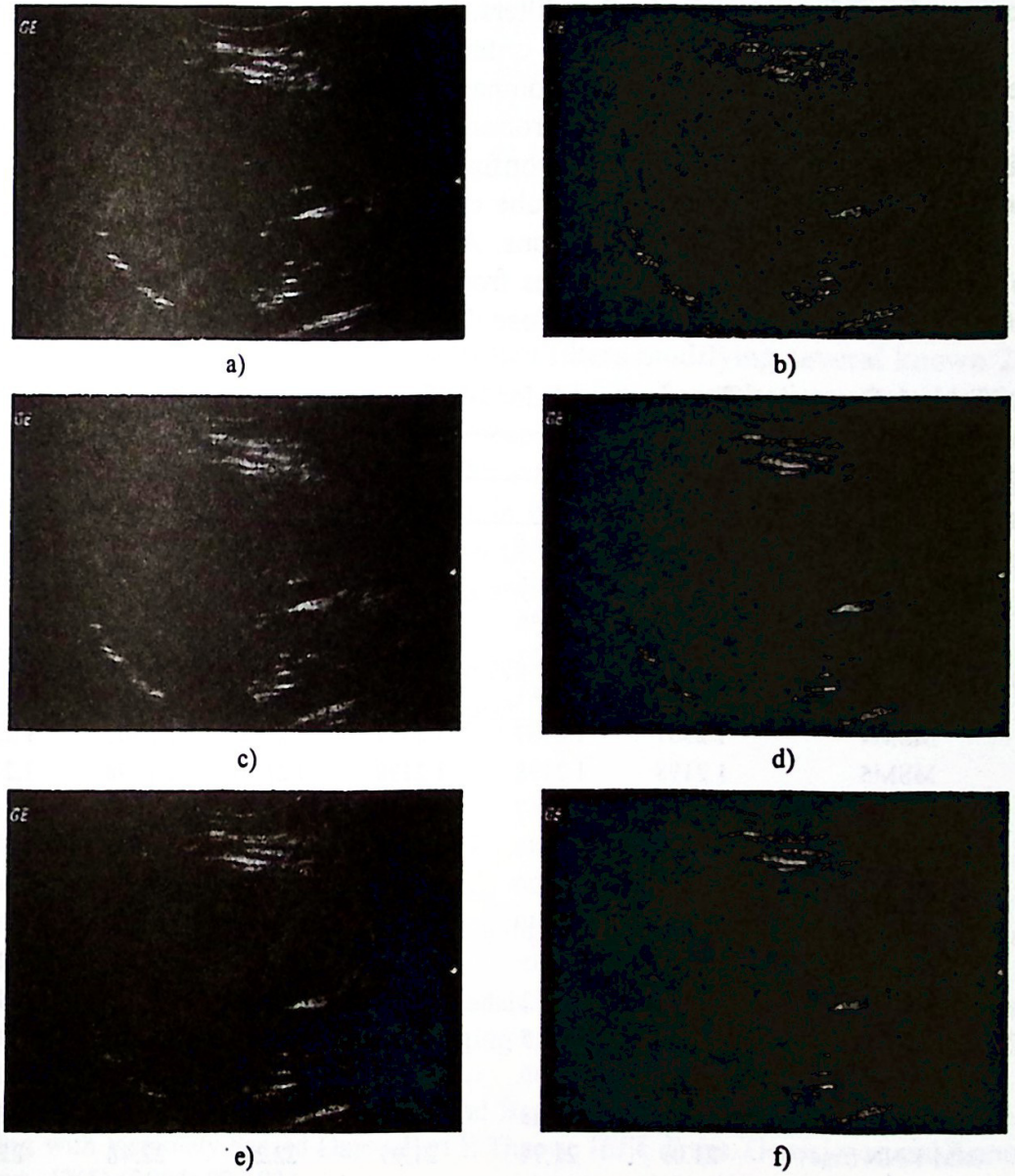

Figure 3. Visual results obtained by MM-KNN filter with the use of different cube configurations in a frame of ultrasound sequence degraded with 30 % of impulsive noise, a) original image, b) degraded image, c) restored image by *a* cube, d) restored image by *d* cube, e) restored image by *g* cube, f) restored image by *i* cube.

The experiment 4 was realized using an ultrasound sequence of 525x382x12 image voxels. The sequence was degraded with 5, 10, 15, 20, 25, and 30% of impulsive noise. Table 4 show the processing time values in seconds for the proposed filters and other filters used as comparative in a frame of ultrasound sequence. The processing time includes the time to acquisition, processing, and storing data.

One can see from the Table 4 that the processing time for Selection Median and Average filters have sufficiently small time values. These filters use the technique that permits dividing the cube into two groups calculating the mean and median fastly, but for LUM Smooth, LUM Sharp y LUM filters the time values are increased during the ordering stage of 27 voxels. The processing time values for RM-KNN filters are large in comparison other filters. It is easy to see that processing time values are increased but the performance criteria PSNR and MAE are sufficiently better (see Table 1) for RM-KNN filters in comparison with other known ones.

Finally, in the experiment 5 we processed the ultrasound sequence as in the experiment 4 using the different cube configurations. Table 5 displays the processing time values in seconds for different cube configurations in the MM-KNN filter with the Hampel and Cut influence functions. Analyzing this table we can conclude that applying the cube voxel configurations from *a* to *f*, it is possible to decrease significantly the processing time and do not lose the quality of filtering (see Table 3).

Table 4. Processing Time in seconds for 3-D filtering in the case of impulsive noise.

3-D Filters	Impulsive noise percentage					
	5%	10%	15%	20%	25%	30%
α Trimmed Mean	2.1716	2.1716	2.1716	2.1716	2.1716	2.1716
Ranked Order	1.6836	1.6836	1.6836	1.6836	1.6836	1.6836
MSM1	0.5846	0.5846	0.5846	0.5846	0.5846	0.5846
MSM2	0.5773	0.5773	0.5773	0.5773	0.5773	0.5773
MSM3	1.2681	1.2681	1.2681	1.2681	1.2681	1.2681
MSM4	1.2367	1.2367	1.2367	1.2367	1.2367	1.2367
MSM5	1.2198	1.2198	1.2198	1.2198	1.2198	1.2198
MSM6	1.1667	1.1667	1.1667	1.1667	1.1667	1.1667
MaxMed	1.1981	1.1981	1.1981	1.1981	1.1981	1.1981
SelAve	1.9620	1.9620	1.9620	1.9620	1.9620	1.9620
SelMed	2.3240	2.3240	2.3240	2.3240	2.3240	2.3240
LUM Smooth	4.122	4.705	5.355	5.754	6.047	7.123
LUM Sharp	4.224	4.812	5.469	5.867	6.165	7.257
LUM	4.317	4.915	5.582	5.984	6.285	7.402
MM-KNN Cut	20.49	20.59	20.61	20.63	20.66	20.87
MM-KNN Hamp.	2051	20.53	21.02	21.26	21.26	21.75
MM-KNN Sine	21.09	21.74	21.99	22.24	22.48	22.71
MM-KNN Berno.	21.94	22.01	22.25	22.49	22.73	22.98
MM-KNN Tukey	21.71	21.74	21.76	21.77	22.26	22.74
WM-KNN Cut	39.78	42.49	44.91	44.92	44.99	45.17
WM-KNN Hamp.	38.54	40.19	42.62	45.06	46.05	47.55
ABSTM-KNN Cut	31.15	32.39	32.44	36.80	37.07	39.70
ABSTM-KNN Hamp.	34.14	35.52	36.63	38.00	38.08	42.13

Table 5. Processing time for the MM-KNN filters in the case of different cube configurations.

Voxel configuration	MMKNN (Hampel)			MMKNN (Cut)		
	Impulsive Noise Percent					
	10	20	30	10	20	30
a	1.763	1.787	1.812	1,594	1.643	1.659
b	2.053	2.077	2.101	1.866	1.908	1.916
c	4.618	4.635	4.692	4.807	4.823	4.872
d	4.696	5.201	5.264	4.754	5.199	5.252
e	4.66	4.628	4.690	4.804	4.816	4.869
f	4.616	4.642	4.693	4.800	4.830	4.871
g	9.939	10.04	10.06	10.06	10.06	10.06
h	9.969	10.02	10.04	10.05	10.07	10.08
i	21.02	21.26	21.75	20.61	20.66	20.87

5 Conclusions

We have investigated novel 3-D order statistics filters modifying several known 2-D ones for 3-D imaging. The experimental system, which allows the investigation of the 3-D objects in the ultrasound imaging has been designed. The RM-KNN filters have the better performance in the most of cases suppressing the impulsive and speckle noise, and preserving the fine-scale details in 3-D images. Different proposed cube configurations of the voxels investigated in the paper permit to obtain the compromise between filtering quality performances and processing time.

Acknowledgements. The authors thank the National Polytechnic Institute of Mexico and CONACYT (project 42790) for its support.

References

1. Webb, A. G. Introduction to Biomedical Imaging. Wiley-IEEE Press. Hoboken, New Jersey (2002)
2. Abd-Elmoniem, K. Z., Youssef, A. M. & Kadah, Y. M. Real-Time Speckle Reduction and Coherence Enhancement in Ultrasound Imaging via Nonlinear Anisotropic Diffusion. IEEE Trans. Biomed. Eng. 49(9) (2002) 997-1014.
3. Shkvarko, Y. V. Unifying Regularization and Bayesian Estimation Methods for Enhanced Imaging with Remotely Sensed Data---Part I: Theory. IEEE Trans. Geoscience and Remote Sensing. 42(5) (2004) 923-931.
4. Shkvarko, Y. V. Unifying Regularization and Bayesian Estimation Methods for Enhanced Imaging with Remotely Sensed Data---Part II: Implementation and Performance Issues. IEEE Trans. Geoscience and Remote Sensing. 42(5) (2004) 932 -940.
5. Porter, B. C., Rubens, D. J., Strang, J. G., Smith, J., Totterman, S. & Parker, K. J. Three-Dimensional Registration and Fusion of Ultrasound and MRI Using Major Vessels as Fiducial Markers. IEEE Trans. Med. Imag. 20(4) (2001) 354-359.

6. Shekhar, R. & Zagrodsky, V. Mutual Information-Based Rigid and Nonrigid Registration of Ultrasound Volumes. IEEE Trans. Med. Imag. 21(1) (2002) 9-22.
7. Nikolaidis, N. & Pitas, I3-D Image processing algorithms, John Wiley & Sons, New York (2000)
8. Bovik, A. Handbook of Image and Video Processing. Academic Press. San Diego CA (2000)
9. Astola, J. & Kuosmanen, P. Fundamentals of Nonlinear Digital Filtering. CRC Press. Boca Raton-New York (1997)
10. Kotropoulos, C. & Pitas, I. Nonlinear Model-Based Image/Video Processing and Analysis, John Wiley & Sons, New York (2001)
11. Pitas, I. & Venetsanopoulos, A. N. Nonlinear Digital Filters: Principles and Applications, Kluwer Academic Publisher, Boston (1990)
12. Kim, J. S. & Park, H. W. Adaptive 3-D median filtering for restoration of an image sequence corrupted by impulsive noise, Signal Processing: Image Communication. 16 (2001) 657-668.
13. Texas Instruments TMS320C6711,TMS320C6711B, TMS320C6711C Floating-Point Digital Signal Processors, SPRS088H: Texas Instruments Incorporated (2003)
14. Texas Instruments TMS320C6000 Optimizing Compiler User's Guide, SPRU187G. Dallas: Texas Instruments Incorporated (2000)
15. Texas Instruments TMS320C6000 Code Composer Studio Tutorial, SPRU301C. Dallas: Texas Instruments Incorporated (2000)
16. Gallegos-Funes, F. J. & Ponomaryov V. I. Real-time image filtering scheme based on robust estimators in presence of impulsive noise. Real Time Imaging, 8(2) (2004) 78-90.
17. Gallegos-Funes, F., Ponomaryov, V. & De-La-Rosa, J. ABST M-type K-nearest neighbor (ABSTM-KNN) for image denoising. IEICE Trans. Fundamentals of Electronics, Communications and Computer Sciences. E88-A(3) (2005) 798-799
18. Ponomaryov, V. I., Gallegos-Funes, F. J. & Sansores-Pech R. Real-Time 3D ultrasound imaging. Proc. SPIE Real-Time Imaging IX. Vol. 5671 (2005) 19-29
19. Hampel, F. R., Ronchetti, E. M., Rouseew, P. J. & Stahel, W. A. Robust Statistics. The approach based on influence function. Wiley, New York (1986)
20. Crinon, R. J. The Wilcoxon filter: a robust filtering scheme. Proc. IEEE Int. Conf. Acoust., Speech, and Signal Process. 85 (1985) 668-671
21. Microchip EEPROM Memory Programming Specification, DS30282E: Microchip Technology Incorporated (2002)
22. Bednar, J. B. & Watt, T. L. Alpha-trimmed means and their relationship to median filters. IEEE Trans. Acoust., Speech, and Signal Process. ASSP-32 (1984) 145-153.
23. Arce, G. R. Multistage order statistic filters for image sequence processing. IEEE Trans. Signal Process. 39(5) (1991) 1146-1163.
24. Nieminen, A. & Neuvo, Y. Comments of theoretical analysis of the max/median filter. IEEE Trans. Acoust., Speech, and Signal Process. ASSP-36 (1988) 826-827.
25. Hardie, R. C. & Boncelet, C. G. LUM filters: a class of rank order based filters for smoothing and sharpening. IEEE Trans. Signal Process. 41 (1993) 1061-1076.